

Dependence of the pyroelectric response on internal stresses in ferroelectric thin films

Z.-G. Ban and S. P. Alpay^{a)}

Department of Metallurgy and Materials Engineering and Institute of Materials Science University of Connecticut, Storrs, Connecticut 06269

(Received 13 February 2003; accepted 24 March 2003)

The role of internal stresses on the pyroelectric properties of ferroelectric thin films is analyzed theoretically via a thermodynamic model. The pyroelectric coefficient as a function of the misfit strain is calculated for (001) Ba_{0.6}Sr_{0.4}TiO₃ epitaxial thin films. It is shown that this property is highly dependent on the misfit strain. A very large pyroelectric response (0.65 μC/cm²K) is theoretically predicted at a critical misfit strain (~-0.05%) corresponding to the ferroelectric to paraelectric phase transformation. The analysis shows that internal tensile stresses are particularly not desirable with significant degradation close to an order of magnitude in the pyroelectric response. © 2003 American Institute of Physics. [DOI: 10.1063/1.1576503]

In recent years, there is a continuing growth of interest in pyroelectric materials for IR detection and thermal imaging applications.¹ Unlike semiconductor or photon detectors, pyroelectric IR detectors can operate at ambient temperatures, thereby eliminating the need for expensive multistage thermal regulation systems. The task of designing more economical IR detection devices with a better performance has led to the use of ferroelectric thin films as potential candidates as the operational component of such devices.²⁻⁴ In particular, the integration of hybrid arrays of ferroelectric thin films detectors with silicon readout integrated circuits (ICs) can offer a high performance for infrared imaging.^{5,6}

Compared to bulk ceramic or single crystals, ferroelectric materials in thin film form are characterized by the presence of compositional and microstructural inhomogeneities, defects, and internal stresses. These factors are believed to be the reason for the inferior electrical and electromechanical properties observed in ferroelectric thin films. For epitaxial single-domain ferroelectric thin films, the role of internal stresses on the electrical and electromechanical properties has been determined experimentally.⁷⁻⁹ It was shown that the dielectric and piezoelectric response strongly depends on internal stresses. Indeed, close to an order of magnitude variation in these properties has been observed when the internal stress levels were systematically altered upon using various substrate materials with a variety of film thickness.^{7,10} Ferroelectric thin films also exhibit a significantly inferior pyroelectric behavior compared to their bulk ceramic or single crystal counterparts of the same composition. Recent experimental studies show that the pyroelectric coefficients routinely observed in the barium strontium titanate (BST) and lead zirconate titanate (PZT) thin films for IR detectors are in the range of 0.03–0.3 μC/cm²K,^{2,3,11,12} nowhere close to the theoretically predicted pyroelectric coefficients of BST and PZT single crystals (typically above 1 μC/cm²K near the Curie temperature).

It is, therefore, of great technological and scientific importance to understand the role of internal stresses on the

pyroelectric response of ferroelectric thin films. In this letter, we study the role of the epitaxy-induced internal stresses (or the misfit strain) on the pyroelectric properties of epitaxial single-domain (001) BST films. We extend the theoretical methodology first developed by Pertsev *et al.*¹³ based on a Landau–Ginzburg–Devonshire phenomenology to analyze the pyroelectric response of ferroelectric thin films. This approach has recently been applied to investigate the dielectric response and the tunability of epitaxial BST films.¹⁴ For this analysis, we concentrate on Ba_{0.6}Sr_{0.4}TiO₃ (BST 60/40) which is a promising pyroelectric material due to the proximity of its Curie temperature ($T_C=2^\circ\text{C}$) to RT (25 °C), resulting in a high IR response at RT.¹⁵ The aim of this letter is to provide a quantitative estimation for the dependence of the pyroelectric properties on epitaxy-induced internal stresses as to serve as a guide for future experimental studies.

Consider a single-domain (001)-oriented ferroelectric film deposited in the cubic paraelectric state on a thick (001) cubic substrate. The thermodynamic potential \tilde{G} can be expressed in terms of the polarization P_i , the applied field E_i , and the misfit strain $u_m = (a_S - a_0)/a_S$, where a_S is the substrate lattice parameter and a_0 is the cubic cell constant of the free standing film, and is given by^{13,14}

$$\begin{aligned} \tilde{G} = & a_1^*(P_1^2 + P_2^2) + a_3^*P_3^2 + a_{11}^*(P_1^4 + P_2^4) + a_{33}^*P_3^4 \\ & + a_{13}^*(P_1^2P_3^2 + P_2^2P_3^2) + a_{12}^*P_1^2P_2^2 \\ & + a_{111}(P_1^6 + P_2^6 + P_3^6) + a_{112}[P_1^4(P_2^2 + P_3^2) \\ & + P_3^4(P_1^2 + P_2^2) + P_2^4(P_1^2 + P_3^2)] + a_{123}P_1^2P_2^2P_3^2 \\ & + \frac{u_m^2}{S_{11} + S_{12}} - (E_1P_1 + E_2P_2 + E_3P_3). \end{aligned} \quad (1)$$

The vector and tensor quantities are defined in a Cartesian coordinate system such that for example, $P_1 \parallel [100]$, $P_2 \parallel [010]$, and $P_3 \parallel [001]$. The renormalized coefficients of the free energy expansion in Eq. (1) are

^{a)}Electronic mail: p.alpay@ims.uconn.edu

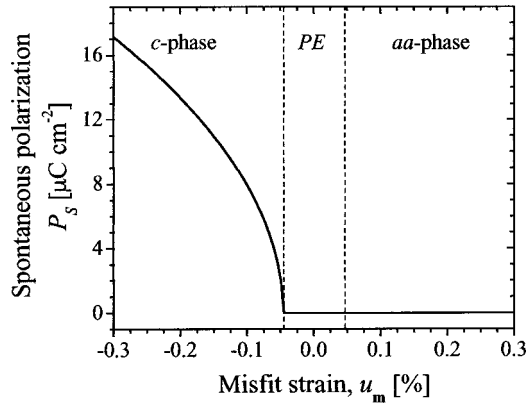


FIG. 1. The spontaneous polarization P_S as a function of the misfit strain u_m for BST 60/40 epitaxial thin films in the absence of electric field ($E=0$) at room temperature. Dashed vertical lines show the stability regions of phases with respect to the misfit strain (PE: paraelectric phase).

$$\begin{aligned}
 a_1^* &= a_1 - u_m \frac{Q_{11} + Q_{12}}{S_{11} + S_{12}}, & a_3^* &= a_1 - u_m \frac{2Q_{12}}{S_{11} + S_{12}}, \\
 a_{11}^* &= a_{11} + \frac{1}{2} \frac{1}{S_{11}^2 - S_{12}^2} [(Q_{11}^2 + Q_{12}^2)S_{11} - 2Q_{11}Q_{12}S_{12}], \\
 a_{33}^* &= a_{11} + \frac{Q_{12}^2}{S_{11} + S_{12}}, \\
 a_{12}^* &= a_{12} - \frac{1}{S_{11}^2 - S_{12}^2} [(Q_{11}^2 + Q_{12}^2)S_{12} - 2Q_{11}Q_{12}S_{11}] \\
 &\quad + \frac{Q_{44}^2}{2S_{44}}, \\
 a_{13}^* &= a_{12} + \frac{Q_{12}(Q_{11} + Q_{12})}{S_{11} + S_{12}},
 \end{aligned} \tag{2}$$

where a_1 is the dielectric stiffness, a_{ij} and a_{ijk} are higher order stiffness coefficients at constant stress, Q_{ij} are the electrostrictive coefficients, and S_{ij} the elastic compliances of the film. The temperature dependence of the dielectric stiffness a_1 is given by the Curie–Weiss law, $a_1 = (T - T_0)/2\epsilon_0 C$, where T_0 and C are the Curie–Weiss temperature and constant of a bulk ferroelectric, respectively, and ϵ_0 is the permittivity of free space. The change in the symmetry due to the mechanical boundary conditions results in six possible phases compared to three phases in ferroelectric single crystals.¹³ The analysis of stability of various phases yields a phase diagram in the plane of temperature and misfit strain. For epitaxial (001) BST 60/40 films, it has been shown that only the c phase ($P_1 = P_2 = 0, P_3 \neq 0$), the paraelectric phase ($P_1 = P_2 = P_3 = 0$), and the aa phase ($P_1 = P_2 \neq 0, P_3 = 0$) are stable at room temperature (see Fig. 1 of Ref. 14). Large compressive stresses favor the formation of the c -phase, while the large tensile stresses stabilize the aa phase.

There are two primary pyroelectric modes for infrared detection by the ferroelectric film: conventional mode and dielectric mode,¹ although variations combining the two effects are also commonly used. The conventional or intrinsic mode utilizes the rapid change in spontaneous polarization with temperature in the region of the paraelectric-ferroelectric phase transition. The radiation induces change

in the detector temperature thereby resulting in a change of polarization equivalent to the flow of a surface charge. The dielectric or the dielectric bolometer mode requires the IR detector to operate above or close to the transition temperature in the presence of an applied electric field. In this mode, the spontaneous polarization is absent or very small and the variation of dielectric permittivity by incident heating gives rise to a detectable signal voltage. BST is best known for its infrared detection applications as a dielectric bolometer material for barium compositions in the 40%–70% range. For example, bulk stress-free BST 60/40 is intrinsically paraelectric with no spontaneous polarization at room temperature. However, in epitaxial BST 60/40 thin films there may be an intrinsic pyroelectric response as internal compressive stresses stabilize the ferroelectric c phase by shifting the paraelectric-ferroelectric phase transition temperature and thereby giving rise to an out-of-plane spontaneous polarization $P_3 = P_S$ at RT. This behavior is illustrated in Fig. 1 where we plot the spontaneous polarization P_S as a function of the misfit strain u_m for BST 60/40 epitaxial thin films in the absence of an electric field at RT. The parameters used for the calculation of the renormalized coefficients for BST films are obtained by averaging the corresponding parameters of BaTiO₃ and SrTiO₃.¹⁶ The aa phase, although ferroelectric, does not possess a component of polarization along the film-substrate normal. The spontaneous polarization P_S for the c phase in the absence of an electric field is given by¹⁴

$$P_S = \sqrt{-a_3^*/2a_{33}^*}. \tag{3}$$

Unlike bulk BST 60/40, epitaxial BST 60/40 films are intrinsically ferroelectric for negative misfit strains larger than -0.05% . Therefore, epitaxial BST 60/40 film under compressive stresses can exhibit intrinsic pyroelectric properties. Furthermore, a gradual decrease of the spontaneous polarization is predicted as the misfit strain increases, eventually resulting in a c phase to paraelectric phase transformation around -0.05% . A sharp increase in the pyroelectric response should be expected at this critical misfit strain due to the ferroelectric to paraelectric phase transformation.

At a constant applied field along the film-substrate normal ($E = E_3$), the pyroelectric coefficient p is given by¹⁷

$$p = \left(\frac{\partial D}{\partial T} \right)_E = \frac{\partial P_S}{\partial T} + E \frac{\partial \epsilon}{\partial T}, \tag{4}$$

where D is the dielectric displacement and ϵ is the permittivity. The first term in Eq. (4) for the c phase can be obtained by taking the first derivative of spontaneous polarization given in Eq. (3) with respect to temperature as

$$\frac{\partial P_S}{\partial T} = \frac{\partial P_3}{\partial T} = -\frac{\sqrt{2}}{4} (-a_3^* a_{33}^{*3})^{-1/2} \left(a_{33}^* \frac{\partial a_3^*}{\partial T} - a_3^* \frac{\partial a_{33}^*}{\partial T} \right), \tag{5}$$

where P_3 is the polarization along the film/substrate interface normal at zero field. It should be noted that the first term in Eq. (4) for paraelectric phase and aa phase are zero since there is no out-of-plane spontaneous polarization component

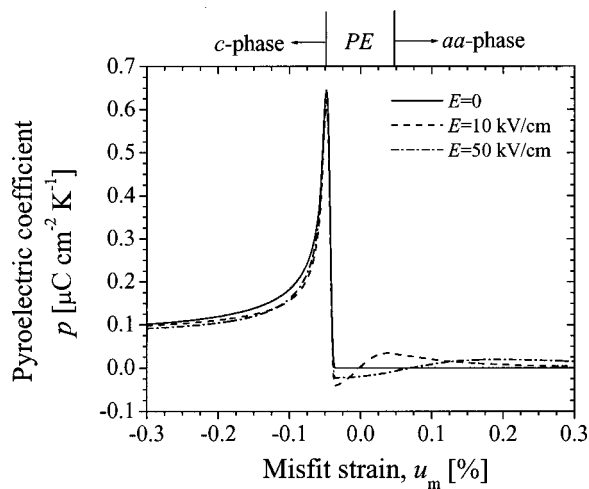


FIG. 2. The pyroelectric coefficient p as a function of misfit strain u_m for BST 60/40 epitaxial thin films at electric field $E=0, 10, 50$ kV/cm at room temperature.

for either phase. The second term in Eq. (4) can be obtained by analyzing the field dependent dielectric permittivity ϵ given by¹⁴

$$\epsilon(E) = \epsilon_3(E) = \left(\frac{\partial^2 \tilde{G}}{\partial P_3^2} \right)^{-1} = \frac{1}{2[a_3^* + a_{13}^*(P_1^2 + P_2^2) + 6a_{33}^*P_3^2]}, \quad (6)$$

where the polarization P_i ($i=1,2,3$) is determined through the condition of equilibrium $\partial \tilde{G} / \partial P_i = 0$.¹⁴

Figure 2 shows the calculated pyroelectric coefficient p as a function of misfit strain u_m for BST 60/40 epitaxial thin films for $E=E_3=0, 10, 50$ kV/cm. It can be seen that the internal stresses have a pronounced effect on the pyroelectric coefficient in BST ferroelectric thin films. In the c -phase region, both spontaneous polarization and dielectric permittivity contribute to the pyroelectric response and an increase of misfit strain results in a decrease of the pyroelectric coefficient. A maximum pyroelectric coefficient is predicted at the critical misfit strain ($\sim -0.05\%$) corresponding to the transformation of the c phase to the paraelectric phase. In the c -phase region, the effect of the applied field on the pyroelectric coefficient is small due to the overwhelming contribution of spontaneous polarization to the overall pyroelectric coefficient. An interesting finding from Fig. 2 is that tensile stresses significantly deteriorate the pyroelectric response. For $u_m > -0.05\%$, only dielectric permittivity contributes to the pyroelectric coefficient as there is no spontaneous polarization. The small pyroelectric response in this region is due to the relatively small rate of change in the dielectric permittivity with temperature.

Any device application based on the pyroelectric properties of ferroelectric materials is critically dependent on the successful integration of these materials with the Si-based technology of ICs. However, deposition of ferroelectric films on Si wafers creates problems beyond the synthesis. Due to the large difference in the lattice parameters between Si (5.431 Å) and BST 60/40 (3.960 Å), very high internal ten-

sile stresses results. Epitaxial growth cannot be achieved and films deposited on Si are usually polycrystalline. Furthermore, since the film growth is usually carried out at high temperatures, high tensile internal stresses develop during cooling down to RT due to the very large difference in the thermal expansion coefficients of Si ($\sim 2.6 \times 10^{-6} \text{ }^\circ\text{C}^{-1}$) and BST ($\sim 10.5 \times 10^{-6} \text{ }^\circ\text{C}^{-1}$). Although there are no epitaxy-induced stresses for polycrystalline BST films deposited on Si, thermal stresses should result in a variation in the phase transformation temperature, stabilizing the paraelectric phase and thereby significantly reducing the pyroelectric response. One way of mitigating the effect of internal stresses for films deposited upon Si is by depositing one or more appropriately selected buffer layers.¹⁸ The buffer layers should be chosen such a way that the ferroelectric film should be in in-plane compression at the deposition temperature as to compensate for the tensile thermal stresses that will develop as the heterostructure is cooled to ambient temperatures. Another possible solution to this problem would be to delineate the film into ferroelectric “islands” with lateral (in-plane) dimensions less than the film thickness.¹⁹ These islands are virtually stress free and mechanically unconstrained.

This work was supported by the National Science Foundation (NSF) under Grant No: DMR-0132918 and the University of Connecticut Research Foundation. The authors gratefully acknowledge helpful conversations with Joseph V. Mantese of Delphi Research Laboratories.

¹R. Watton, *Ferroelectrics* **91**, 87 (1989).

²J.-G. Cheng, J. Tang, J.-H. Chu, and A.-J. Zhang, *Appl. Phys. Lett.* **77**, 1035 (2000).

³C. Shi, M. Liu, L. C. , Y. Zeng, and J. D. Costa, *Thin Solid Films* **375**, 288 (2000).

⁴C. Björmander, K. Scenivas, A. M. Grishin, and K. V. Rao, *Appl. Phys. Lett.* **67**, 58 (1995).

⁵J. V. Mantese, A. L. Micheli, N. W. Schubring, A. B. Catalan, K. L. Soch, K. Ng, S. H. Kapper, R. J. Lopez, and G. Lung, *IEEE Trans. Electron Devices* **40**, 320 (1993).

⁶E. Wiener-Avneer, *Appl. Phys. Lett.* **65**, 1784 (1994).

⁷C. L. Canedy, H. Li, S. P. Alpay, L. Salamanca-Riba, A. L. Roytburd, and R. Ramesh, *Appl. Phys. Lett.* **77**, 1695 (2000).

⁸V. Nagarajan, S. P. Alpay, C. S. Ganpule, B. Nagaraj, S. Aggarwal, E. D. Williams, A. L. Roytburd, and R. Ramesh, *Appl. Phys. Lett.* **77**, 438 (2000).

⁹L. A. Knauss, J. M. Pond, J. S. Horwitz, D. B. Chrissy, C. H. Mueller, and R. Treece, *Appl. Phys. Lett.* **69**, 25 (1996).

¹⁰H. Li, A. L. Roytburd, S. P. Alpay, T. D. Tran, L. Salamanca-Riba, and R. Ramesh, *Appl. Phys. Lett.* **78**, 2354 (2001).

¹¹T.-J. Zhang and H. Ni, *Sens. Actuators A* **100**, 252 (2002).

¹²W.-G. Liu, J. S. Ko, and W.-G. Zhu, *Thin Solid Films* **371**, 254 (2000).

¹³N. A. Pertsev, A. G. Zembilgotov, and A. K. Tagantsev, *Phys. Rev. Lett.* **80**, 1988 (1998).

¹⁴Z.-G. Ban and S. P. Alpay, *J. Appl. Phys.* **91**, 9288 (2002); **93**, 504 (2003).

¹⁵R. W. Whatmore, P. C. Osbond, and N. M. Shorrocks, *Ferroelectrics* **76**, 351 (1987).

¹⁶The parameters used for the calculation of Figs. 1 and 2 (in SI units, T in $^\circ\text{C}$): $a_1^* = 4.63 \times 10^5(T-5) - 1.90 \times 10^{10}u_m$, $a_3^* = 4.63 \times 10^5(T-5) + 1.96 \times 10^{10}u_m$, $a_{11}^* = 2.16T \times 10^6 + 1.44 \times 10^9$, $a_{33}^* = 2.16T \times 10^6 + 7.95 \times 10^8$, $a_{12}^* = 1.73 \times 10^8$, $a_{13}^* = 1.51 \times 10^8$; data compiled from Z.-G. Ban and S. P. Alpay, *J. Appl. Phys.* **91**, 9288 (2002); **93**, 504 (2003).

¹⁷A. M. Glass, *J. Appl. Phys.* **40**, 4699 (1969).

¹⁸Y. Wang, C. Ganpule, B. T. Liu, H. Li, K. Mori, B. Hill, M. Wuttig, R. Ramesh, J. Finder, Z. Yu, R. Droopad, and K. Eisenbeiser, *Appl. Phys. Lett.* **80**, 97 (2002).

¹⁹A. L. Roytburd, S. P. Alpay, V. Nagarajan, C. S. Ganpule, S. Aggarwai, E. D. Williams, and R. Ramesh, *Phys. Rev. Lett.* **85**, 190 (2000).